

# Zonal Flows and GAMs in Comparative Gyrokinetic and Two-Fluid Tokamak Turbulence Simulations

K. Hallatschek<sup>1</sup>

<sup>1</sup>Max-Planck-Institute for Plasma Physics, Garching, Germany

*Corresponding Author:* Klaus.Hallatschek@ipp.mpg.de

## 1 Introduction

Gyrokinetic simulations have come to be the standard of current turbulence modelling in the low gradient, nearly collisionless region in the core of tokamak discharges, since they include nearly all the kinetic effects to be expected for a small ratio of the turbulence to the Larmor frequency [1]. On the other hand, fluid turbulence computations allow much higher spatial resolution, become more reliable at large collision frequency, can be adapted to non-Boussinesq scenarios and tend to yield more physical insight than fully kinetic simulations. The large ratios of domain size to vortex diameter accessible by fluid simulations are also relevant to the study of deterministic zonal flow (ZF) interactions. At present the full nonlinearities that become relevant at the notoriously difficult edge region of tokamaks due to the high fluctuation amplitude cannot be implemented in a gyrokinetic framework. In addition the high collision numbers at the edge make gyrokinetic simulations numerically and physically challenging.

To allow a more reliable operation of both approaches in their respective fringe regions of validity and applicability, and to isolate special kinetic effects from the more robust fluid physics, results on ZF [2] and geodesic acoustic modes (GAM) [3, 4, 5] obtained with the non-local two-fluid Braginskii code NLET have been compared with gyrokinetic code simulations. The specific study of the global flows is of particular interest, with a view towards an eventual understanding of the L/H transition and the associated edge flows.

## 2 Geodesic acoustic modes

In non-marginal regions, far from instability thresholds, the results of the fluid code are in rather good agreement with the kinetic results, even if the collisions are scarce. This can be understood, because at sufficiently large growth rates, the resonances responsible for fine phase space structures become sufficiently wide to allow a representation by fluid moments of the distribution functions.

For example for the parameters  $\epsilon_n = 2L_n/R = 0.08 \Leftrightarrow R/L_n = 25$ ,  $\eta_i = L_n/L_{Ti} = 3$ ,  $q = 3.2$ ,  $\epsilon = a/R = 0.2$ ,  $q = 3.2$  in the core/edge transitional regime and for collisionless ions and adiabatic electrons the ITG modes are far above the threshold for the fluid as well as the kinetic model. In addition the typical mode frequencies of order of the diamagnetic

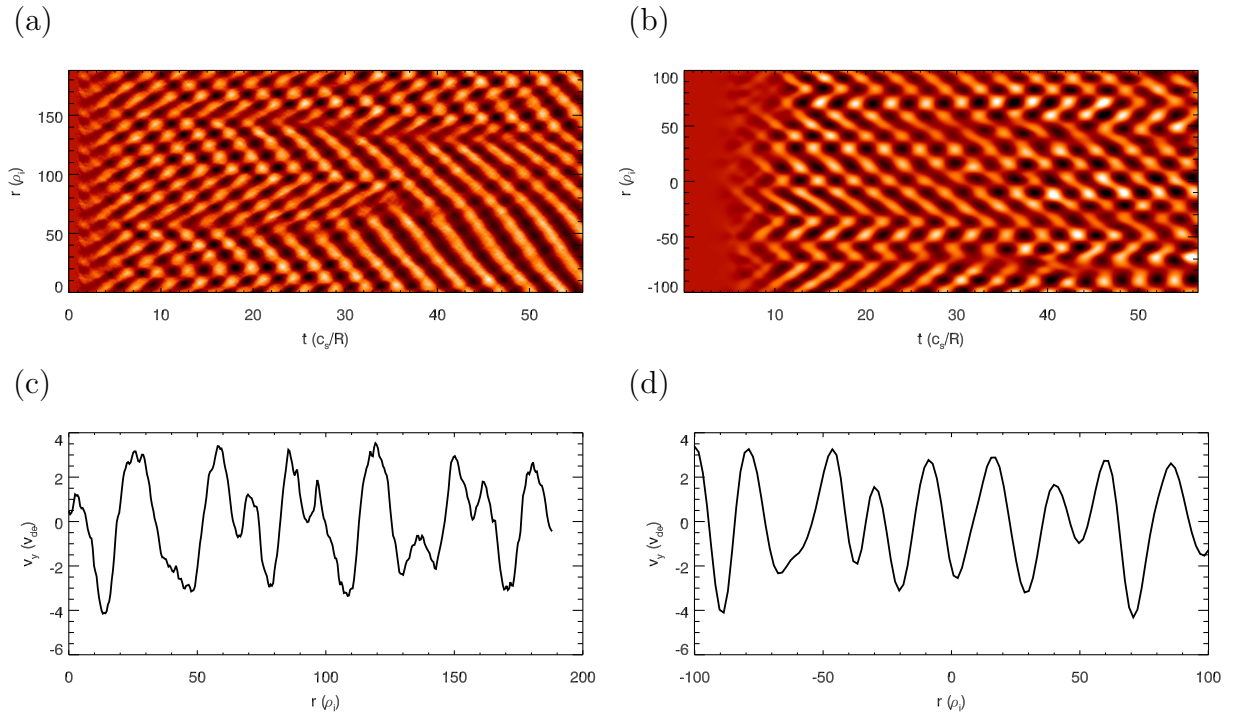


FIG. 1: Figure a and b, respectively, show the profiles of the flux surfaced averaged flow velocity as a function of minor radius and time for the gyrokinetic and the fluid code runs in the core/edge transitional regime, while inset c and d show snapshots of the flow profiles at  $t = 21$  and  $t = 28$ . For better visual comparison, for the fluid run only half the radial domain is shown. (The actually used radial domain width was twice the one in the gyrokinetic code.)

frequency are larger than the magnetic drift frequencies by a ratio of order  $\epsilon_n^{-1}$ . The diamagnetic frequency is also much larger than the parallel ion sound transit time by a ratio  $4\pi q\epsilon_n^{-1}$  – in other words, the turbulence is strongly supersonic. This rules out a large contribution from resonant particle populations due to parallel or perpendicular drifts.

A comparison of the GAM oscillations of the flux surface averaged poloidal velocity for these parameters is shown in figure 1 using the gyrokinetic GYRO [8] and the two-fluid NLET [9] code. The amplitude, pattern, time- and length-scales of the flows agree rather well, indicating that kinetic effects due to higher moments of the distribution function (which are absent in the fluid code) are unimportant in this scenario.

Also the heat flux modulation seen ubiquitously in fluid GAM/turbulence simulations [7] can be observed in the gyrokinetic runs (fig. 2). It is noteworthy, that in both cases the transport maxima are *in phase* with the poloidal flow velocity, where the electron diamagnetic direction counts as positive.

### 3 Zonal Flows

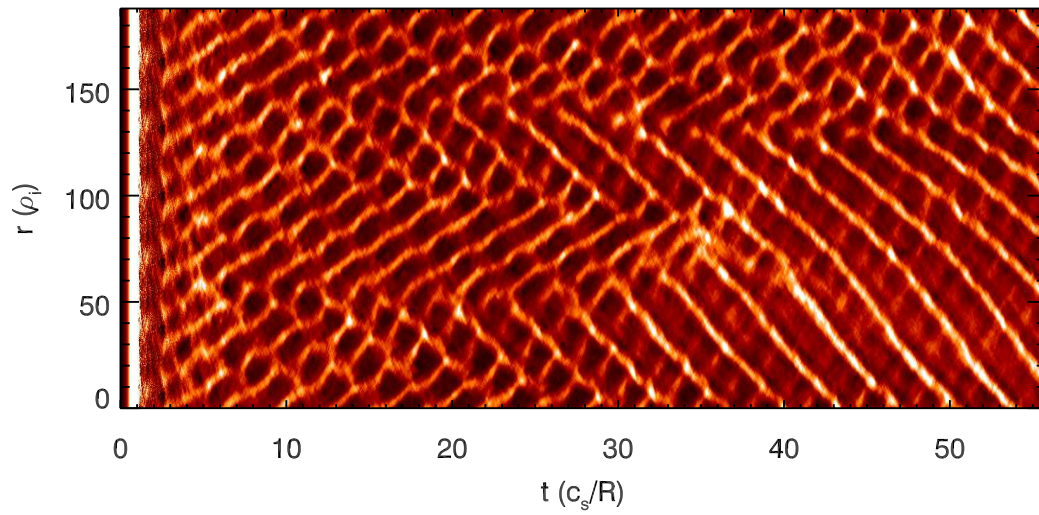
A pronounced feature of the ZFs in many fluid runs [10] is a slowly, nearly deterministically evolving flow, which is maintained by the perpendicular Reynolds stress and braked by the parallel stress acting on the associated  $m = 1$  return flow. The return flow contains the dominant part of the kinetic energy [2]. Gyrokinetic simulations so far have not emphasized the deterministic nature of this flow, as they have focused mostly on the transport level.

A particular challenge of matching fluid and gyrokinetic simulations is the fact that fluid simulations do not depend on the aspect ratio  $\epsilon = a/R$ . An obvious way how this might matter in gyrokinetic simulations is via the banana neoclassical enhancement of the polarizability associated with the ZFs,  $\rho_{eff}/\rho = 1 + 1.6q^2/\sqrt{\epsilon}$ , for circular low aspect ratio discharges. This must be compared to the fluid neoclassical enhancement  $\rho_{eff}/\rho = 1 + 2q^2$ . It seems at first, that particularly low values of  $\epsilon$  might lead to large kinetic deviations from the fluid behavior. This is however attenuated by the fact that the bounce period of the ions causing the increased polarizability also becomes very long for small  $\epsilon$ . These ions become irrelevant, as soon as the setup time of the flows due to the turbulence becomes shorter than their bounce period. For particularly large  $\epsilon$  on the other hand, the kinetic value for the polarizability is limited below by the fluid value, since that value corresponds to the sole contribution of the parallel velocity moment to the kinetic energy of the flows.

For the parameters  $\epsilon_n = 1$ ,  $L_n/L_T = \eta_i = 2.4$ ,  $q = 1.5$ ,  $\epsilon = a/R = 0.2$  the time evolution of the flow profiles in a gyrokinetic turbulence simulation are shown in figure 3a-d. The radial scale (flow wavelength of about  $80\rho_s$  is apparently independent of the radial domain width and the peak flow amplitude about  $0.8v_{dia}$ . The flow velocity agrees approximately with the corresponding fluid value, while the radial scale length is somewhat larger.

To really observe deterministic behavior of the flows the poloidal domain width is clearly not enough. However switching to a larger  $\epsilon = 0.4$  results already in a nearly deterministic flow behavior at unchanged domain. Interestingly, in this case the flow amplitude and the scale length approximately agree with the fluid results, which is understandable, since the neoclassical inertia is closer to the limiting fluid one.

(a)



(b)

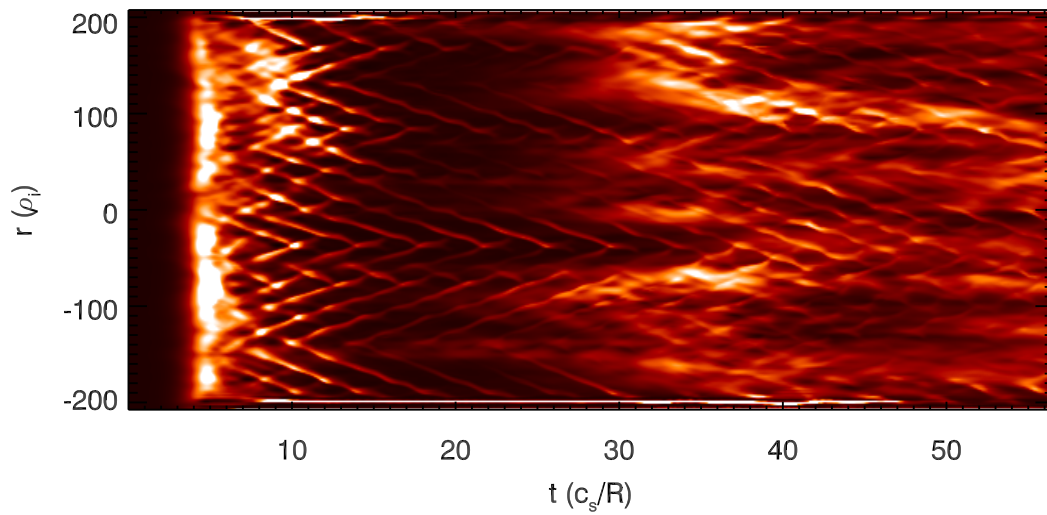


FIG. 2: Figure a and b, respectively, show the profiles of the flux surfaced averaged radial heat flux as a function of minor radius and time for the gyrokinetic and the fluid code runs in the core/edge transitional regime. (Note the different scaling of the radial axis.)

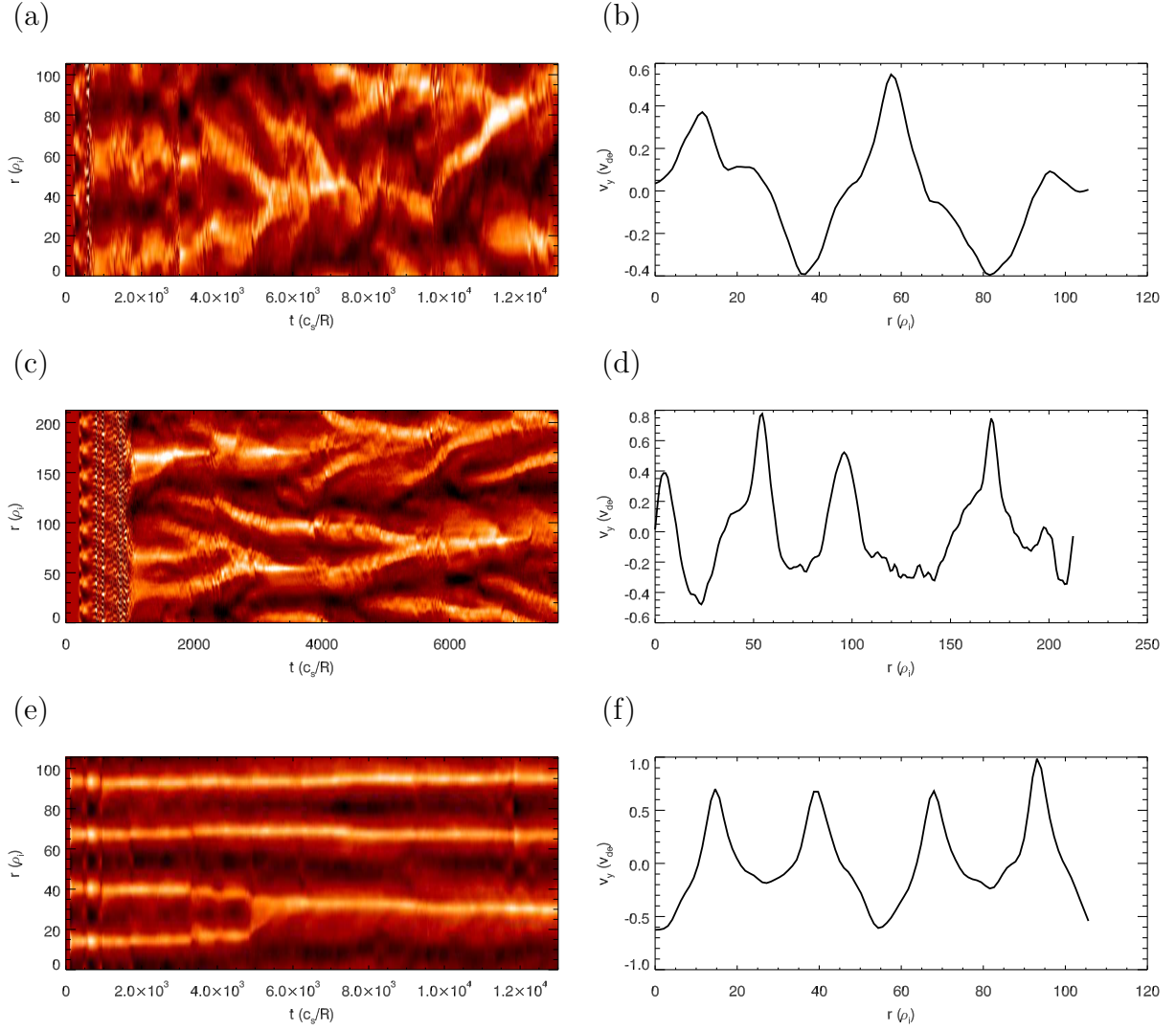


FIG. 3: Figure a and b, respectively, show the profile of the flux surfaced averaged flow velocity as a function of minor radius and time and at  $t = 3280$  for a gyrokinetic run with stationary ZFs for  $\epsilon = a/R = 0.2$  for a perpendicular computational domain of  $107\rho_s \times 168\rho_s$ , and for figure c and d, respectively for a domain of  $213\rho_s \times 168\rho_s$ . Figure e and f show the same flux surface average profiles and snap shots for  $\epsilon = a/R = 0.4$  for a domain of  $107\rho_s \times 168\rho_s$ .

## 4 Conclusions

The comparisons show that ZFs are generated similarly by a Reynolds stress based self amplification and interact with the turbulence modes through wave kinetic effects, while GAMs mostly result from a modulation of the background diamagnetic velocity. Several prior results from the fluid code have been confirmed with the gyrokinetic codes, such as near-deterministic flow evolution for large enough domain sizes, turbulence modulation by GAMs, and stationary behavior of slab-drift-wave generated ZFs.

An important caveat raised by the comparisons is that particular care has to be taken with the physics and numerics of the collision operator used in the gyrokinetic codes, so that the proper fluid limit is eventually reached for high collisionalities. On the other hand, the gyrokinetic results can guide the proper renormalization of the fluid dissipative terms to account for the kinetic damping mechanisms (Landau-damping and phase-mixing) to prevent a partial break-down of the fluid description at the lower collisionalities.

Major differences in the flows are caused by the collisionless modifications to the neo-classical polarizability due to ion trapping. These effects tend to be negligible, if either the aspect ratio or the ratio of turbulent diffusion time versus the ion bounce period is small. The deviations due to the non-adiabatic electron behavior due to trapping in the kinetic code become less important for the high collision numbers often encountered approaching the edge. Lastly, at perpendicular wave-lengths of the order of the ion gyro-radius there are deviations due to the fluid ion polarizability (if the turbulence saturates by inertial and not other dissipative effects). In principle, this requires correction terms to the fluid ion inertia, but becomes less important in non-marginal situations, where the turbulence is dominated by large scale modes. Interestingly the fluid polarization term becomes correct again at very high wave-numbers, where the ions become adiabatic in both frameworks.

The regions of validity and renormalizations of the fluid and gyrokinetic codes outlined by the present paper can be used to study regions close to the edge, where the gyrokinetic ordering breaks down, such as near the L/H transition or the density limit, and are a valuable sanity check for both approaches. Lastly, the presented results improve the understanding of the physics when kinetic phenomena can be reproduced in first principle fluid codes.

## Acknowledgement

A part of this work was carried out using the HELIOS supercomputer system at IFERC-CSC, Aomori, Japan. A part of this work has been carried out within the framework of the EUROfusion Consortium and has received funding from the Euratom research and training programme 2014-2018 under grant agreement No 633053. The views and opinions expressed herein do not necessarily reflect those of the European Commission.

- [1] R.E. Waltz, Zhao Deng, *Phys. Plasmas* **20**, 012507 (2013)
- [2] K. Hallatschek, *Plasma Phys. Control. Fusion* **49**, B137–B148 (2007)
- [3] R. Hager, K. Hallatschek, *Phys. Plasmas* **16**, (2009) 072503
- [4] R. Hager, K. Hallatschek, *Plasma Phys. Control. Fusion* **55**, 035009 (2013)
- [5] K. Hallatschek, G. R. McKee, *Phys. Rev. Lett.* **109**, 245001 (2012)
- [6] A. Zeiler, et al., *Phys. Plasmas* **5**, (1998) 2654
- [7] K. Hallatschek, *Phys. Rev. Lett.* **86**, 1223 (2001)

- [8] J. Candy, R.E. Waltz, J. Comput. Phys. **186**(2), 545 (2003)
- [9] K. Hallatschek, A. Zeiler, Phys. Plasmas **7**, (2000) 2554
- [10] K. Hallatschek, Phys. Rev. Lett. **93**, 065001 (2004)